



Contents lists available at ScienceDirect

Materials Today: Proceedings

journal homepage: www.elsevier.com/locate/matpr

Bio-inspired synthesis of PbO nanoparticles (NPs) via an aqueous extract of *Rosmarinus officinalis* (rosemary) leaves

S.K. Noukelag^{a,b,c,*}, H.E.A. Mohamed^{a,b}, L.C. Razanamahandry^d, S.K.O. Ntwampe^{e,f}, C.J. Arendse^c

^a UNESCO-UNISA Africa Chair in Nanosciences-Nanotechnology Laboratories (U2AC2N), College of Graduate Studies, University of South Africa (UNISA), Muckleneuk Ridge, PO Box 392, Pretoria, South Africa

^b Nanosciences African Network (NANOAFNET), Material Research Department (MRD), iThemba LABS-National Research Foundation, 1 Old Faure Road, Somerset West 7129, PO Box 722, Somerset West, Western Cape, South Africa

^c Department of Physics and Astronomy, University of the Western Cape, Robert Sobukwe Road, Private Bag X17, Bellville 7535, South Africa

^d African Union Development Agency, Economic Integration Division, PO Box 1685, Johannesburg, South Africa

^e Bioresource Engineering Research Group (BioERG), Cape Peninsula University of Technology, PO. Box 652, Cape Town 8000, South Africa

^f School of Chemical Engineering, North West University, Potchefstroom Campus Private Bag X6000, Potchefstroom 2520, South Africa

ARTICLE INFO

Article history:

Received 22 August 2019

Received in revised form 26 April 2020

Accepted 28 April 2020

Available online xxxxx

Keywords:

Bio-inspired synthesis

α -PbO

β -PbO

Nanoparticles

Rosmarinus officinalis (rosemary)

Extract

Electron microscopy

ABSTRACT

There is a pressing need for the development of nanoparticles (NPs) for environmental nanoscience and nanotechnology. Bio-inspired synthesis of lead oxide nanoparticles has been successfully demonstrated using an aqueous extract of *Rosmarinus officinalis* (rosemary) leaves. Structural and optical investigations of lead oxide annealed at 600 °C were carried-out using complementary techniques namely, X-ray diffraction (XRD) that showed the formation of both form α -PbO (tetragonal) and β -PbO (orthorhombic) NPs with the average crystalline size found approximately at 8.96 nm whereas field emission scanning electron microscopy (FESEM) revealed NPs highly agglomerated with the average particle size found to peak at 12.69 ± 0.27 nm. Energy dispersive X-ray spectroscopy (EDS) confirmed the high purity of PbO as well as attenuated total reflection-Fourier transform infrared spectroscopy (ATR-FTIR) and Raman spectroscopy. From UV-Vis-NIR, the energy bandgap has amounted to 4.44 eV and the photoluminescence (PL) emission spectrum showed broad nature of visible emissions peaks at 361, 448, 562 and 689 nm with high surface defects and oxygen vacancies. Through these findings, the use of Rosemary leaves extract is hereby shown to be a cost-effective and environmentally benign alternative to synthesize lead oxide nanoparticles (PbO NPs).

© 2020 Elsevier Ltd. All rights reserved.

Selection and peer-review under responsibility of the scientific committee of the NANOSMATAFRICA-2018.

1. Introduction

Being multifunctional, metal oxides present a rich area of research because of their attractive physico-chemical properties. Their interface and bio-conjugation capabilities provide innovative avenues for fabricating nano-scaled matter with novel and advanced properties. With the ongoing developments on the multi-disciplinary aspect of nanoscience, metal oxide nanoparticles have gained significant popularity for the development of new and effective strategies in biomedicine [1–3].

The lead element has several oxide forms including PbO, Pb₂O₃, PbO₂, and Pb₃O₄. Lead oxide is a semiconductor that exists in two crystalline forms: the alpha-form generally referred to litharge (red-tetragonal) and the beta-form which is commonly known as massicot (yellow-orthorhombic) [4,5]. Due to their unique properties, lead oxides have wide applications such as luminescent materials, gas sensors, storage devices, acid batteries, paints, lead glasses, lead glazes, lead crystals, and in decorative potteries [6,7]. Overall, there is a need for simplicity in design, low input cost of synthesis, reliability, and relative safety as well as the requirement for more greener and environmentally benign synthesis [8,9].

Nanomaterials properties may be engineered by controlling their size, shape, and morphology via chemical, physical or biological synthesis methods; however, the use of chemical and physical methods of synthesis for lead oxide nanoparticles is disadvantageous due to the hazardous waste generation (Chemistry based)

* Corresponding author at: Department of Physics and Astronomy, University of the Western Cape, Robert Sobukwe Road, Private Bag X17, Bellville 7535, South Africa.

E-mail address: sandrinedoum@yahoo.fr (S.K. Noukelag).

Table 1
Major chemical composition of rosemary leaves natural extract [13].

Chemical composition	Explanation
FLAVONOIDS	PELARGONIDIN-3,5-DIGLUCOSIDE (I) CYANIDIN-3,5DIGLUCOSIDE(II) KAEMPFEROL (III)
MONOTERPENOIDS	α - PINENE (IV) 1,8-CINEOLE CAMPHOR
PHENOLIC ACIDS	ROSMARINIC ACID CAFFEIN ACID
DITERPENOIDS	CARNOSOL METHYL CARNOSATE 12-METHOXYCARNOSIC ACID EPI- AND ISO-ROSMANOL

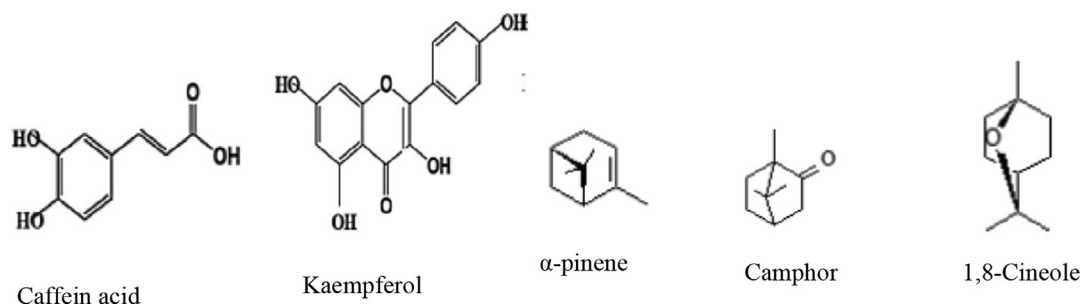


Fig. 1. Structure of major bioactive molecular compounds in rosemary leaves extract.

and not cost-effectiveness (Physical based) [4–7]. On the contrary, phytosynthesis using plant extracts is favored as it can overcome such disadvantages while imparting environmental benignity with the synthesis green, simple and less energy intensive with minimal waste generated, thus an economical synthesis route to produce the desired metal oxides nanoparticles [2,8,9]. Plant extracts phytoexudes can be used as capping and/or reducing agents for a green chemistry nanoparticles synthesis. The size, shape, and morphology of the nanoparticles can be controlled [2,10,14]. To the best of our knowledge, bioinspired synthesis of lead oxide using rosemary leaves extract that facilitates the capping and stabilization of nanoparticles during synthesis has never been researched.

Rosemary is an aromatic medicinal and condiment plant that belongs to the family Labiate. The medicinal uses of rosemary are well documented, and it is mostly used in the treatment of jaundice, hepatitis, circulatory, and cardiovascular diseases [11,12]. Bioactive components in rosemary extracts include phenolic compounds including other constituents (see Table 1) can play a critical role in the capping and stabilization of nanoparticles [12,13].

Furthermore, Fig. 1 depicts the structure of major bioactive molecular compounds of rosemary leaves extract.

In this study, a completely green synthesis procedure for two phases lead oxide using leaves extract of the medicinal plant rosemary (*Rosmarinus officinalis*) is reported. Bioinspired synthesis of lead oxide using rosemary leaves extract and characterization is reported herein in this study for the first time.

2. Synthesis: Green process via rosemary leaves natural extract

2.1. Bioinspired synthesis

Rosemary leaves were purchased from a nursery (Western Cape Province, Cape Town–South Africa). Lead acetate $Pb(CH_3COO)_2$ was purchased as an analytical grade reagent (Sigma Aldrich, Modderfontein, South Africa).

10 g of rosemary leaves were weighed and washed with sterile distilled water at ambient temperature. Subsequently, they were immersed in 200 mL of deionized water to extract phytoexudes, a process achieved by boiling at 80 °C for 2 h. The resultant

phytoextracts' pH was found to be 5.7. The extract solution was filtered twice to eliminate residual solids, after the addition of 6 g/100 mL extracts of the precursor salt, i.e. lead acetate, was homogeneously mixed at 80 °C for 1 h. Thereafter, a slight acidification of the resultant solution was observed, with a final pH of 4.6. During the heating phase, the precipitate formation was observed. The resultant solution was allowed to cool to ambient temperature. The precipitate PbO was kept in a drying oven at 100 °C for one day. The dried powder was annealed in a ceramic crucible at 600 °C in an open-air furnace for 2 h leading to nanoparticles of a highly crystalline character that changed color from green to brown.

2.2. Characterizations

Various techniques were used to characterize and investigate the structural and optical properties of the PbO nanoparticles annealed at 600 °C. FESEM using Zeiss Ultra 55 Scanning Electron Microscope was used to study the morphology and shape of the so generated nanoparticles. An X-ray diffractometer (model Bruker AXS D8 Advance) with an irradiation line $K\alpha_1$ of copper ($\lambda_{CuK\alpha_1} = 1.5406 \text{ \AA}$) operating at a voltage of 40 kV and a current of 35 mA, in the angular range of 20–90° was used to study the crystalline nature of the nanoparticles. Energy dispersive X-ray spectroscopy analysis was carried out to determine the elemental composition of the nanoparticles with an EDS Oxford instrument X-Max solid-state silicon drift detector operating at 20 kV. ATR-FTIR absorption spectrometer (Thermo Nicolet 8700 FTIR spectrometer) was used to analyze the sample in the spectral range 400–4000 cm^{-1} to ascertain the surface coating and the chemical bonding of the nanoparticles. UV–VIS–NIR experiment was also conducted using a Nicolette Evolution 100 Spectrophotometer to analyze the optical properties in the spectral range 200–800 nm. Raman spectrum is recorded from 100 to 500 cm^{-1} with a laser line of 473 nm and an average excitation power of 2.48 mW. Photoluminescence (PL) was recorded from 200 to 1000 nm with a Varian Cary Eclipse Fluorescence Spectrophotometer at an excitation wavelength of 372 nm.

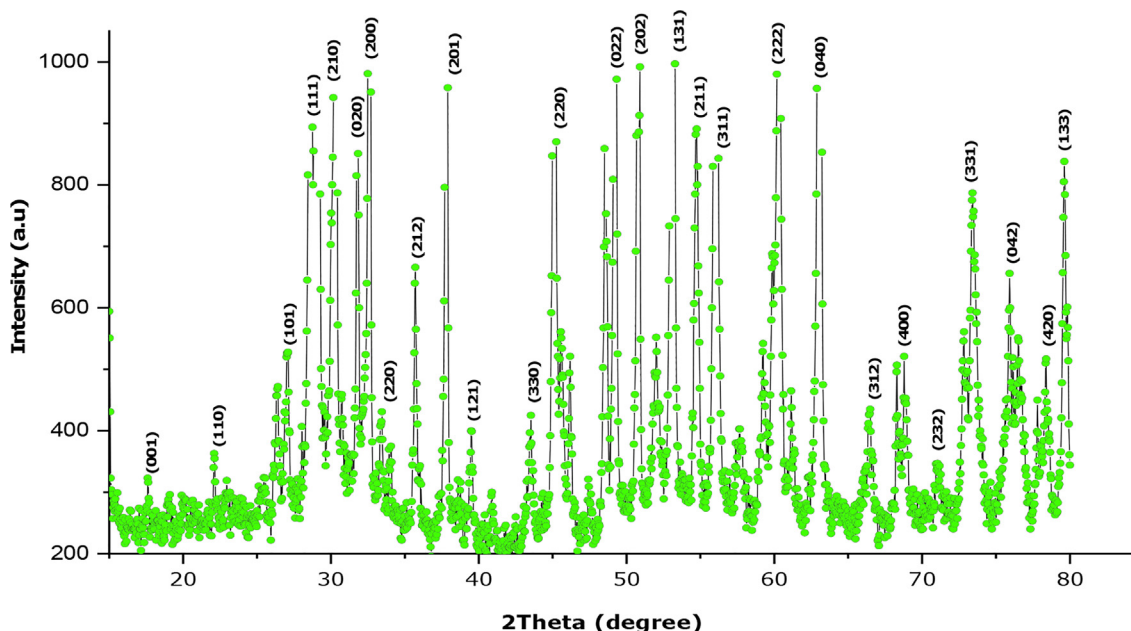


Fig. 2. XRD spectrum of litharge and massicot phases PbO nanoparticles annealed at 600 °C for 2 h.

3. Results and discussion

3.1. Crystallographic analysis

The X-ray diffraction spectrum of the bioinspired synthesis lead oxide nanoparticles is depicted in Fig. 2. The observed Bragg peaks were the crystallographic reflections of orthorhombic massicot and tetragonal litharge of lead oxide (PbO) having standard lattice parameters of $\langle a \rangle = 0.549$ nm, $\langle b \rangle = 0.589$ nm, $\langle c \rangle = 0.475$ nm, $\langle a/b \rangle = 0.931$ nm and $\langle c/b \rangle = 0.806$ nm which are consistent with the JCPDS pattern no. 00-038-1477 for massicot phase, the face-centered cubic lattice belonged to the space group Pcam (57) and $\langle a \rangle = 0.397$ nm, $\langle b \rangle = 0.502$ nm, $\langle a/b \rangle = 0.790$ nm which are consistent with the JCPDS pattern no. 00-005-0561 for a litharge phase. The diffraction patterns of α -PbO NPs and β -PbO NPs were

confirmed with the tetragonal and orthorhombic structures as annealed at 600 °C for 2 h respectively. The sharper XRD peaks indicated a highly crystalline nature of the PbO NPs [9].

The average crystalline size was calculated using Debye-Scherrer's equation $\langle \varnothing \rangle = 0.9\lambda / \Delta\theta \cos(\theta)$. Where λ , is the wavelength used in XRD (1.54056 Å), $\Delta\theta$ and θ are the full width at half maxima (FWHM) and the Bragg's diffraction angle respectively. Using the above-mentioned formula, average size of the optimized PbO NPs was approximately 8.96 nm.

3.2. Morphological measurements

FESEM and EDS results are depicted in Figs. 3 and 4 respectively. Fig. 3 shows the FESEM micrographs of the pure and agglomerated PbO nanoparticles. The obtained nanoparticles were spherical and

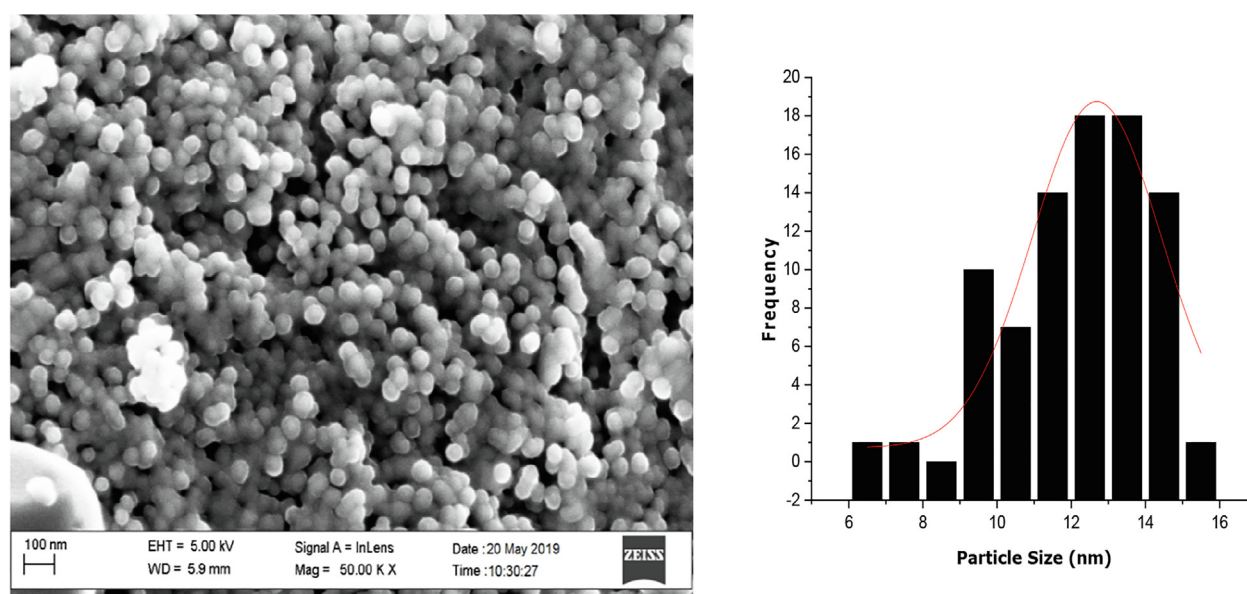


Fig. 3. FESEM micrographs of PbO nanoparticles annealed at 600 °C for 2 h and average size distribution.

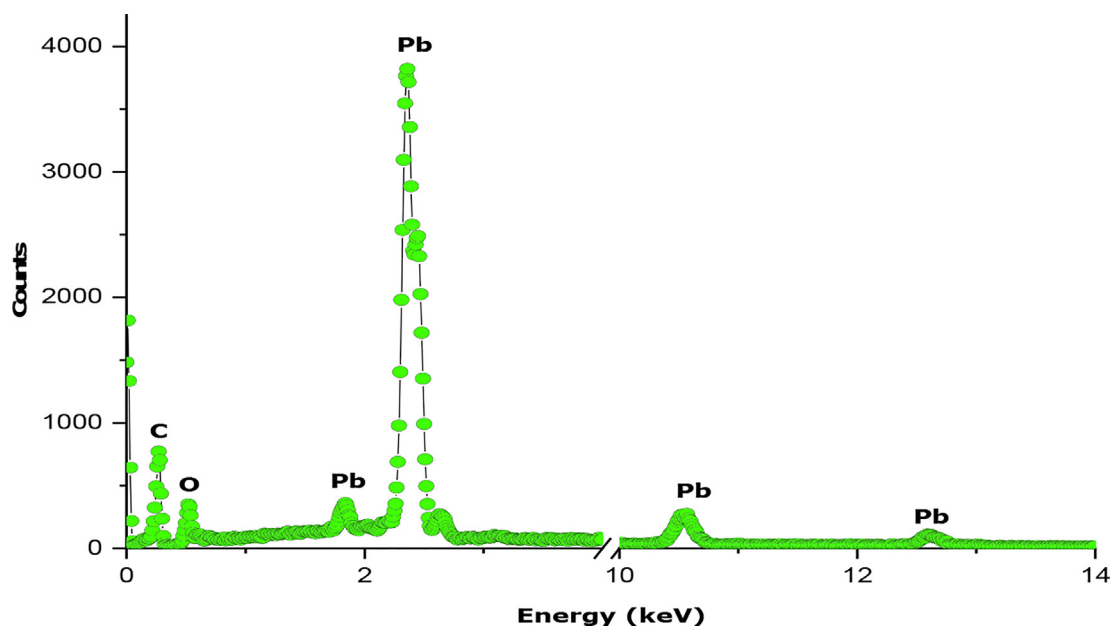


Fig. 4. EDS spectrum of PbO nanoparticles annealed at 600 °C for 2 h.

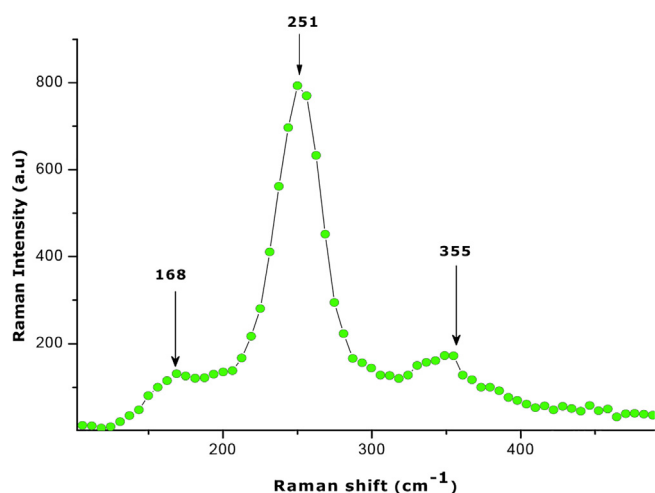


Fig. 5. Raman spectrum of PbO nanoparticles annealed at 600 °C for 2 h.

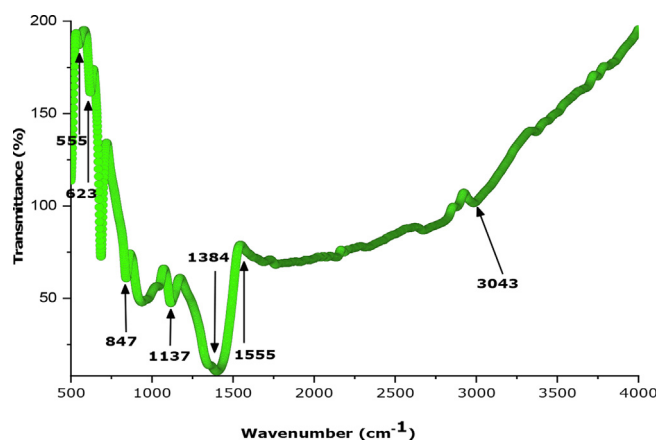


Fig. 6. ATR-FTIR spectrum of PbO nanoparticles annealed at 600 °C for 2 h.

uniform in shape [7,8] and the size was found to be 12.69 ± 0.27 nm.

EDS spectrum of the PbO nanoparticles as depicted in Fig. 4, revealed well-defined peaks identified as characteristic peaks of Pb, with O, confirming the synthesized nanoparticles as lead oxide which is due to its high purity. The peak due to carbon emanates from the carbon tape used as grid support for the PbO nanoparticles.

3.3. Vibrational properties

The vibrational properties for the bioinspired synthesis of litharge and massicot phases lead oxide nanoparticles were studied using Raman spectroscopy, given in Fig. 5. The characteristic peaks of litharge at 251 and 355 cm^{-1} and massicot at 168 cm^{-1} are present in the spectrum. However, the relative positioning of the peaks can change with the difference in the synthesis method used and the distribution vacancies in the unit cell [6].

The crystallinity of the PbO nanoparticles can be pre-concluded because of the intense peak at 251 cm^{-1} .

The vibrational properties for the bioinspired synthesis of litharge and massicot phases lead oxide nanoparticles were also studied using ATR-FTIR as illustrated in Fig. 6. The absorption peaks located at 555, 623, and 847 cm^{-1} indicated the presence of Pb-O stretching modes. These three very sharp peaks confirmed the high purity of the PbO in the sample. The peak at 1384 cm^{-1} indicated the presence of C=O, CH₃, and C=C aromatic functional groups associated with various bioactive compounds in the rosemary leaves extracts. The weak band at 3043 cm^{-1} is associated with hydroxyl groups (—OH) and peaks centered at 1555 and 1137 cm^{-1} indicated functional groups (—C—N—) and (—C—O—) respectively [8,9].

3.4. Optical properties

The absorbance of PbO nanoparticles annealed at 600 °C is carried-out to ratify their presence as elucidated in Fig. 7 with a peak at 235 nm which confirmed the formation of the PbO NPs. The highest peak observed is associated with a charge transfer from the band of conduction to a band of valence cations. The absorbance can slightly increase with further annealing, due to

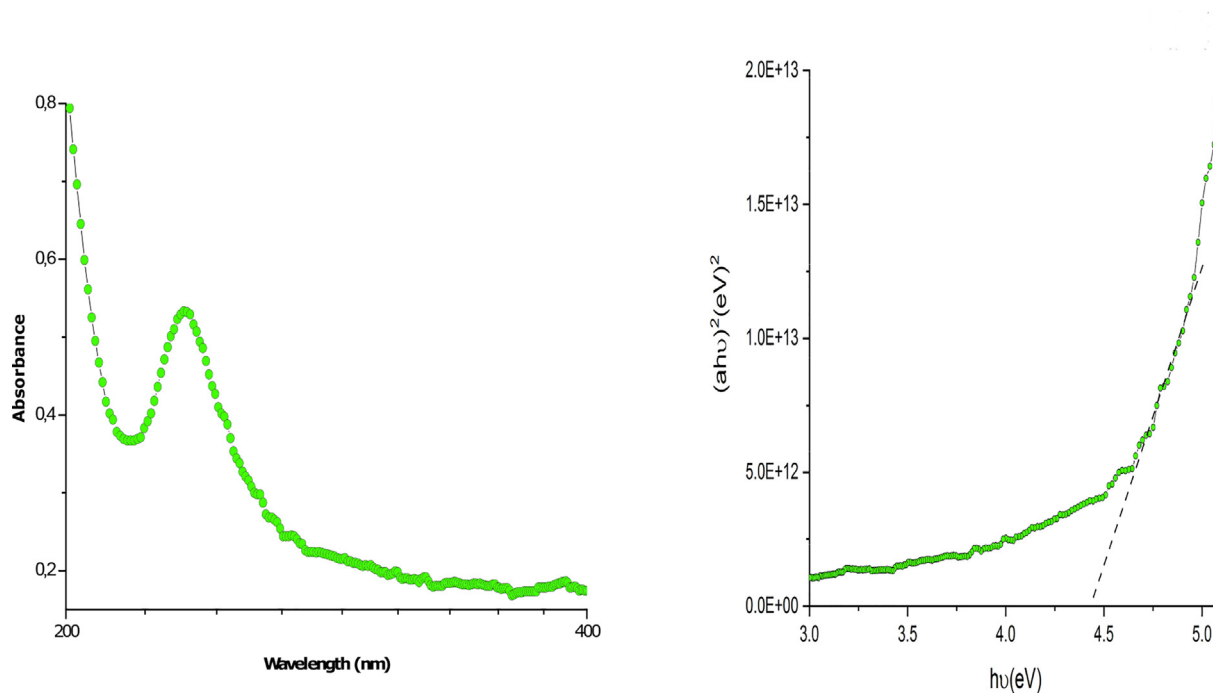


Fig. 7. UV-Visible spectrum of PbO nanoparticles annealed at 600 °C for 2 h.

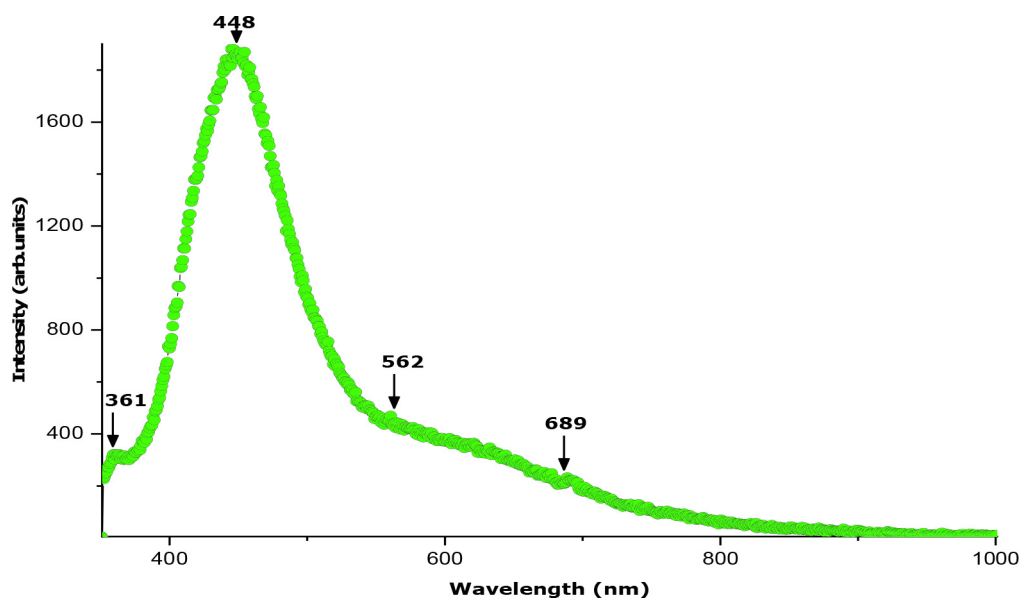


Fig. 8. PL spectrum of PbO nanoparticles annealed at 600 °C for 2 h.

the enhancement of the crystalline quality and larger grain size of the bioinspired synthesis of nanoparticles as evidenced in the XRD analysis and SEM observations. The optical bandgap 'E_g' was calculated using the following well known Tauc's relation $(\alpha h\nu) = A(h\nu - E_g)^n$ where, A is a constant, α is the absorption coefficient, and n is a constant for a given transition which is equal to 1/2 for direct bandgap. 'E_g' was determined by extrapolating the straight portion of the plotted graph to the energy axis at $\alpha = 0$ and was found to be equal to 4.44 eV [7,9].

The photoluminescent spectrum was recorded to understand the effects of quantum size and particle defects. Fig. 8 shows the photoluminescence (PL) spectrum of the PbO NPs annealed at

600 °C with an intense UV emission peak at 361 nm which can be ascribed to band edge emission that results from the recombination of electrons and holes of PbO free excitons. An intense blue emission observed at 448 nm is related to intrinsic defect centers associated with oxygen vacancies. The yellowish-green emission peak at 562 nm can be ascribed also to defects. The red emission peak at 689 nm can be ascribed to multiple oxidation states of lead or the presence of single ionized oxygen vacancies. The visible emissions of the visible spectrum suggest that PbO NPs have a high surface-to-volume ratio with numerous surface-states and defects (vacancies and interstitials) which create trap levels responsible for the emissions observed. The color change of the bioinspired

synthesis of PbO NPs (green to brown) can also be justified by the existence of lead vacancies and/ or interstitial oxygen defects [4,14].

As a follow up of this preliminary and encouraging study, other multifunctional simple and binary oxides, nanoscaled metal & nanocomposites will be biosynthesized using *Rosmarinus officinalis* aqueous leaves extract as an effective chelating agent with their properties, and their applications will be compared to others [15–25].

4. Conclusion

PbO nanoparticles were successfully synthesized via the green chemistry method using *Rosmarinus officinalis* aqueous leaves extract as an effective chelating agent. The various investigations showed that such nano-scaled particles of PbO were polycrystalline within the so-called massicot and litharge phases. Yet the polycrystalline nature, the PbO nanoparticles exhibited a significant population of Oxygen deficiency inducing significant photoluminescence.

CRedit authorship contribution statement

S.K. Noukelag: Conceptualization, Visualization, Investigation, Methodology, Data curation, Writing - original draft, Writing - review & editing. **H.E.A. Mohamed:** Data curation, Writing - review & editing. **L.C. Razanamahandry:** Writing - review & editing. **S.K.O. Ntwampe:** Writing - review & editing. **C.J. Arendse:** Supervision.

Declaration of Competing Interest

The authors declare that they have no known competing financial interests or personal relationships that could have appeared to influence the work reported in this paper.

Acknowledgments

This research program was generously supported by grants from the National Research Foundation of South Africa (NRF), the UNESCO-UNISA Africa Chair in Nanosciences & Nanotechnology, the University of South Africa (UNISA), iThemba LABS-NRF, the Academy of Sciences for the Developing World (TWAS), the University of the Western Cape (UWC) as well as Cape Peninsula University of Technology (CPUT) to whom we are all grateful.

References

- [1] M. Singh, S. Manikandan, A.K. Kumaraguru, Nanoparticles: a new technology with wide applications, *Res. J. Nanosci. Nanotech.* 1 (2011) 1–11.
- [2] M. Ovais, A.T. Khalil, A. Raza, M.A. Khan, I. Ahmad, N.U. Islam, et al., Green synthesis of silver nanoparticles via plant extracts: beginning a new era in cancer theranostics, *Nanomedicine* 12 (23) (2016) 3157–3177.
- [3] K. Arulmozhi, N. Mythili, Studies on the chemical synthesis and characterization of lead oxide nanoparticles with different organic capping agents, *AIP Adv.* 3 (12) (2013) 122122.
- [4] H. Karami, M.A. Karimi, S. Haghdar, et al., Synthesis of lead oxide nanoparticles by sonochemical method and its application as cathode and anode of lead-acid batteries, *Mater. Chem. Phys.* 108 (2–3) (2008) 337–344.
- [5] S.D. Meshram, R.V. Rupnarayan, S.V. Jagtap, V.G. Mete, V.S. Sangawar, Synthesis and characterization of lead oxide nanoparticles, *IJCPS* 4 (2015) 83–84.
- [6] L. Burgio, R.J. Clark, S. Firth, Raman spectroscopy as a means for the identification of plattnerite (PbO₂), of lead pigments and of their degradation products, *Analyst* 126 (2) (2001) 222–227.
- [7] S. D. Meshram, R. V. Rupnarayan, S. V. Jagtap, V. G. Mete, V. S. Sangawar, Synthesis and Characterization of Lead Oxide Nanoparticles, *International Journal of Chemical and Physical Sciences*, ISSN: 2319-6602 IJCPS Vol. 4 Special Issue – NCSC Jan-2015 www.ijcps.org.
- [8] A. Miri, M. Sarani, A. Hashemzadeh, Z. Mardani, M. Darroudi, Biosynthesis and cytotoxic activity of lead oxide nanoparticles, *Green Chem. Lett. Rev.* 11 (4) (2018) 567–572, <https://doi.org/10.1080/17518253.2018.1547926>.
- [9] A.T. Khalil, M. Ovais, I. Ullah, M. Ali, S.A. Jan, Z.K. Shinwari, M. Maaza, Bioinspired synthesis of pure massicot phase lead oxide nanoparticles and assessment of their biocompatibility, cytotoxicity and in-vitro biological properties, *Arabian Journal of Chemistry*, doi: <http://dx.doi.org/10.1016/j.arabjc.2017.08.009>
- [10] B.E.V. Wyk, B.V. Oudtshoorn, N. Gericke, *Medicinal Plants of South Africa*, Briza Publication, Pretoria, South Africa, 2013.
- [11] N. Erkan, G. Ayrançi, E. Ayrançi, Antioxidant activities of rosemary (*Rosmarinus officinalis* L.) extract, blackseed (*Nigella sativa* L.) essential oil, carnosic acid, rosmarinic acid and sesamol, *Food Chem.* 110 (2008) 76–82.
- [12] P.G. Peiretti, F. Gai, M. Ortoffi, R. Aigotti, C. Medana, Effects of Rosemary Oil (*Rosmarinus officinalis*) on the Shelf-Life of Minced Rainbow Trout (*Oncorhynchus mykiss*) during Refrigerated Storage, *Foods* 1 (2012) 28–39, <https://doi.org/10.3390/foods1010028>.
- [13] J. Rafael de Oliveira, S.E.A. Camargo, L. Dias de Oliveira, *Rosmarinus officinalis* L. (rosemary) as therapeutic and prophylactic agent, *J. Biomed. Sci.* (2019), <https://doi.org/10.1186/s12929-019-0499-8>.
- [14] J. Kennedy, P.P. Murmu, E. Manikandan, S.Y. Lee, Investigation of structural and photoluminescence properties of gas and metal ions doped zinc oxide single crystals, *J. Alloys Compd.* 616 (15) (2014) 614–617.
- [15] J.J. Vijaya, N. Jayaprakash, K. Kombaiah, K. Kaviyarasu, L.J. Kennedy, M. Maaza, Bioreduction potentials of dried root of Zingiber officinale for a simple green synthesis of silver nanoparticles: antibacterial studies, *J. Photochem. Photobiol. B Biol.* 177 (2017) 62–68.
- [16] A. Dakka, J. Lafait, C. Sella, S. Berthier, M. Abd-Lefdil, J.C. Martin, M. Maaza, Optical properties of Ag-TiO₂ nanocermet films prepared by co-sputtering and multilayer deposition techniques, *Appl. Opt.* 39 (16) (2000) 2745–2753.
- [17] Zebib.Y. Nuru, C.J. Arendse, R. Nemutudi, O. Nemraoui, M. Maaza, Pt–Al₂O₃ nanocoatings for high temperature concentrated solar thermal power applications, *Phys. B Condensed Matter* 407 (10) (2012) 1634–1637, <https://doi.org/10.1016/j.physb.2011.09.104>.
- [18] M. Maaza, O. Nemraoui, C. Sella, A.C. Beye, Surface plasmon resonance tunability in Au–VO₂ thermochromic nano-composites, *Gold Bull.* 38 (3) (2005) 100–106.
- [19] S.K. Noukelag, H.E.A. Mohamed, B. Moussa, L.C. Razanamahandry, S.K.O. Ntwampe, C.J. Arendse, Structural and optical investigations of biosynthesized bunsenite NiO nanoparticles (NPs) via an aqueous extract of *Rosmarinus officinalis* (rosemary) leaves, *Mater. Today Proc.* (2020), <https://doi.org/10.1016/j.matpr.2020.03.314>, ISSN 2214-7853.
- [20] M. Khenfouch, M. Baïtoul, M. Maaza, White photoluminescence from a grown ZnO nanorods/graphene hybrid nanostructure, *Opt. Mater.* 34 (8) (2012) 1320–1326.
- [21] C.M. Magdalane, K. Kaviyarasu, N. Matinise, N. Mayedwa, N. Mongwaketsi, Evaluation on La₂O₃ garlanded ceria heterostructured binary metal oxide nanoplates for UV/visible light induced removal of organic dye from urban wastewater, *S. Afr. J. Chem. Eng.* 26 (2018) 49–60.
- [22] A.T. Khalil, M. Ovais, I. Ullah, M. Ali, Z.K. Shinwari, S. Khamlich, M. Maaza, *Sageretia thea* (Osbeck.) mediated synthesis of zinc oxide nanoparticles and its biological applications, *Nanomedicine* 12 (15) (2017) 1767–1789.
- [23] J.B.K. Kana, J.M. Ndjaka, B.D. Ngom, N. Manyala, O. Nemraoui, A.Y. Fasasi, Thermochromic nanocrystalline Au–VO₂ composite thin films prepared by radiofrequency inverted cylindrical magnetron sputtering, *Thin Solid Films* 518 (6) (2010) 1641–1647.
- [24] S.K. Noukelag, H.E.A. Mohamed, B. Moussa, L.C. Razanamahandry, S.K.O. Ntwampe, C.J. Arendse, M. Maaza, Investigation of structural and optical properties of biosynthesized Zincite (ZnO) nanoparticles (NPs) via an aqueous extract of *Rosmarinus officinalis* (rosemary) leaves, *MRS Adv.* (2020) 1–10, <https://doi.org/10.1557/adv.2020.220>.
- [25] A.T. Khalil, M. Ovais, I. Ullah, M. Ali, Z.K. Shinwari, M. Maaza, Physical properties, biological applications and biocompatibility studies on biosynthesized single phase cobalt oxide (Co₃O₄) nanoparticles via *Sageretia thea* (Osbeck.), *Arab. J. Chem.* 13 (1) (2020) 606–619.